Sādhanā (2020)45:130
https://doi.org/10.1007/s12046-020-01364-8

© Indian Academy of Sciences

Experimental and FE analysis for the buckling behavior of hat-stiffened panels under edge compressive loading

S KUMAR[1,*], R KUMAR[2] and S MANDAL[2]

[1]Department of Civil Engineering, Sitamarhi Institute of Technology, Sitamarhi, India
[2]Department of Civil Engineering, Indian Institute of Technology (BHU), Varanasi, India
e-mail: Shashi351@gmail.com; rkumar.civ@iitbhu.ac.in; smandal.civ@iitbhu.ac.in

MS received 2 December 2018; accepted 14 April 2020

Abstract. In this paper, experimental studies on two laminated composite hat-stiffened panels with equally spaced stiffeners have been carried out with application of axial compression load on the panel for the determination of the pre-buckling and post buckling behavior. A non-linear buckling analysis on the hat-stiffened panel has also been performed under compression load with application of finite element tool ABAQUS. From strain analysis at different locations, the local buckling of skin has been observed before the buckling of the panel, and a visual damage has been found near the skin-stiffener and debonding skin-stiffener of the panel during failure of the hat-stiffened panel. The compression load-axial displacement curve of the experiments has correlated well with simulated finite element model result for determination of the buckling behavior of the panel up to the failure load. The out of plane displacement pattern shows that the compressive failure initiated at the edges of the panel and gone to skin-stiffener bonding, and finally failure of the panel occurred due to debonding between skin-stiffener.

Keywords. Buckling behavior; hat-stiffened panel; experimental strain analysis; finite element (FE); compression load.

1. Introduction

A lightweight structure is an ongoing task for engineering community, and fiber reinforced polymers do meet some of these requirements. Laminated composite panels have been applied extensively in aircraft, automobiles area, defense and now it is currently employed in structural applications like light weight roof, partition wall and the outer wall of the building. Composite panels are recently applied in historical buildings and bridge for retrofitting of the structures due to its high strength. In stiffened panels, local buckling of plate, global buckling and failure of the panel experience under shear, compression and their combination of compression-shear load cases. The damage of stiffened composite panel initiates from the interface between plate and stiffeners due to stress concentration influenced by deformation of skin and stiffeners after the local buckling of skin of the panel. The buckling behavior of the hat-stiffened panel has been studied under axial compression load by applying non-linear FE method using ABAQUS and experimental work.

Many experimental and numerical studies have been performed on the buckling behavior of stiffened panels under axial compressive loading. Most of the researchers have worked on the laminated composite hat-stiffened panels with I-shaped, blade-type, T-shaped and J-shaped stiffeners. A very few literatures are available on hat-type stiffener of panels. Kong *et al* [1] performed experimental and analytical study on stiffened panel by introducing I-shaped and blade-shaped stiffeners. Bisagni [2] studied the influence of imperfection in shape and amplitude on critical loads of laminated composite cylindrical shells. Lanzi [3] investigated experimental studies on composite stiffened structures subjected to axial load for post-buckling behavior, damage and failure. It was obtained as the imperfections lead to an important reduction in the final failure load of the complex steel silo transition junction structures but the amplitude of the imperfection had small influence on the collapse load of the structure [4, 5]. The initial geometric imperfections had a more effect on the dynamic buckling of the shells, but the sensitivity to initial geometric imperfection depends on the ply configuration of the laminated shells [6]. Bisagni and Cordisco [7] performed experimental study on the buckling and post-buckling of three composite stiffened cylindrical shells. Gal *et al* [8] carried out the experimental studies on graphite-epoxy blade-type stiffened composite panels subjected to axial compression load and observed that all of the specimens were buckled at approximately similar buckling strain. Zimmermann *et al* [9] carried out experimental study

*For correspondence
Published online: 18 May 2020

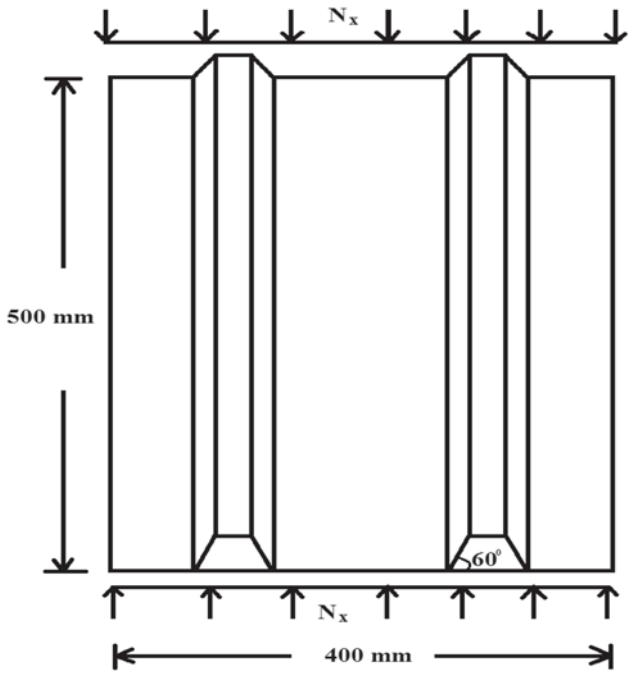

Figure 1. The structural geometry of the hat-stiffened panel.

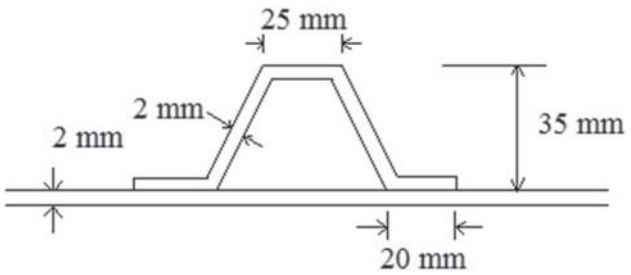

Figure 2. Cross section of the hat-stiffener with plate.

Table 1. Material properties of CFC used in the analysis (SudhirSastry *et al* [17]).

Quantity	Symbol	Units	CFC materials
Young's modulus 0°	E_{11}	GPa	164
Young's modulus 90°	E_{22}	GPa	12.8
Shear modulus in plane 12 and 13	$G_{12} = G_{13}$	GPa	4.5
Shear modulus in plane 23	G_{23}	GPa	2.5
Poisson ratio in plane 12	υ_{12}	–	0.32
Ultimate tensile strength 0°	X_{1t}	MPa	2724
Ultimate compressive strength 0°	X_{1c}	MPa	111
Ultimate tensile strength 90°	X_{2t}	MPa	50
Ultimate compressive strength 90°	X_{2c}	MPa	1690
Ultimate shear strength in plane 12	S_{12}	MPa	120
Ultimate shear strength in plane 13	S_{13}	MPa	137
Ultimate shear strength in plane 23	S_{23}	MPa	60
Density	ρ	Kg/m^3	1800

on buckling behavior of the panels with variation of number of I-shaped stiffeners and its thickness. Pevzner *et al* [10] developed an extended effective width approach to study the bending, torsion and buckling of curved stiffened panels with different types of stiffeners. Orifici *et al* [11] conducted experimental work and studied numerical investigations on collapse behavior of the stiffened structures for damage growth between skin and stiffeners. Elaldi [12] studied laminated composite stiffened panels through experiments and compared post-buckling capacity of hat-shaped and J-shaped stiffened panels. Perret *et al* [13] conducted post-buckling study on composite panel to find out-of-plane displacements with application of two stereo Digital Image Correlation systems located on each side of the panel. Boni *et al* [14] presented experimental and numerical studies on the stiffened panel and compared FE analysis strains with experimental strain gauges result at mid-bay between the stringers. Lui *et al* [15] and Zhu *et al* [16] carried out experimental work to study the buckling load, buckling mode and collapse load of the stiffened panel subjected to compressive loading. SudhirSastry *et al* [17] presented the pre-buckling and post-buckling analysis of stiffened composite panels using ABAQUS based on FE method with carbon fiber and others composite materials. Riccio *et al* [18] and Borrelli *et al* [19] developed kinematic coupling methods for FE model simulation of the buckling behavior on composite I-shaped stiffened structures under

Figure 3. Experimental set-up of hydraulic machine with strain gauge data-logger system.

Figure 4. Specimen of hat-stiffened panel installation.

compression load. Wang *et al* [20] conducted experimental study and found the damage location of the stiffened panel with application of strain gauge at different locations. Kumar *et al* [21] presented an analytical tool artificial neural network for prediction of the buckling load on hat-stiffened panel under axial compression load.

This paper provides the buckling and post buckling behavior of hat-stiffened panels by experimental study and numerical analysis using ABAQUS [22]. Non-linear FE method is used to perform the post buckling behavior of the panel with damage and debonding between the stiffeners and panel.

2. Configurations of the hat-stiffened panel

The structural geometry of the laminated composite hat-stiffened panel is shown in figure 1. Two specimens of panel were tested for experimental studies which are named as panel-A and panel-B. The laminated composite panel was designed with two hat-stiffeners as shown in figure 2. The panel has a width of 400 mm and a length of 500 mm with two hat-stiffeners of spacing 200 mm, depth 35 mm and a fixed top width of 25 mm. Ply configuration $[[45°/-45°/0°/90°/]_s]_s$ of 2 mm thickness of skin laminated sheet was used in all member of the laminated hat-stiffened panel and ply oriented along the direction of stiffener as longitudinal direction of fiber. The material property of carbon fiber composite (CFC) of each ply of thickness 0.125 mm is illustrated in table 1.

3. Experimental set-up

The uniaxial compression test was performed on the stiffened panels by using a universal testing machine with a maximum capability of 400 kN with strain gauge data-logger system as shown in figure 3. For the specimens loading, there are two platforms in the machine. The bottom platform is displaced in a controlled speed, while the top platform is fixed during the tests. The specimen was installed on the test machine as shown in figure 4. The panels were loaded with compression load and clamped in

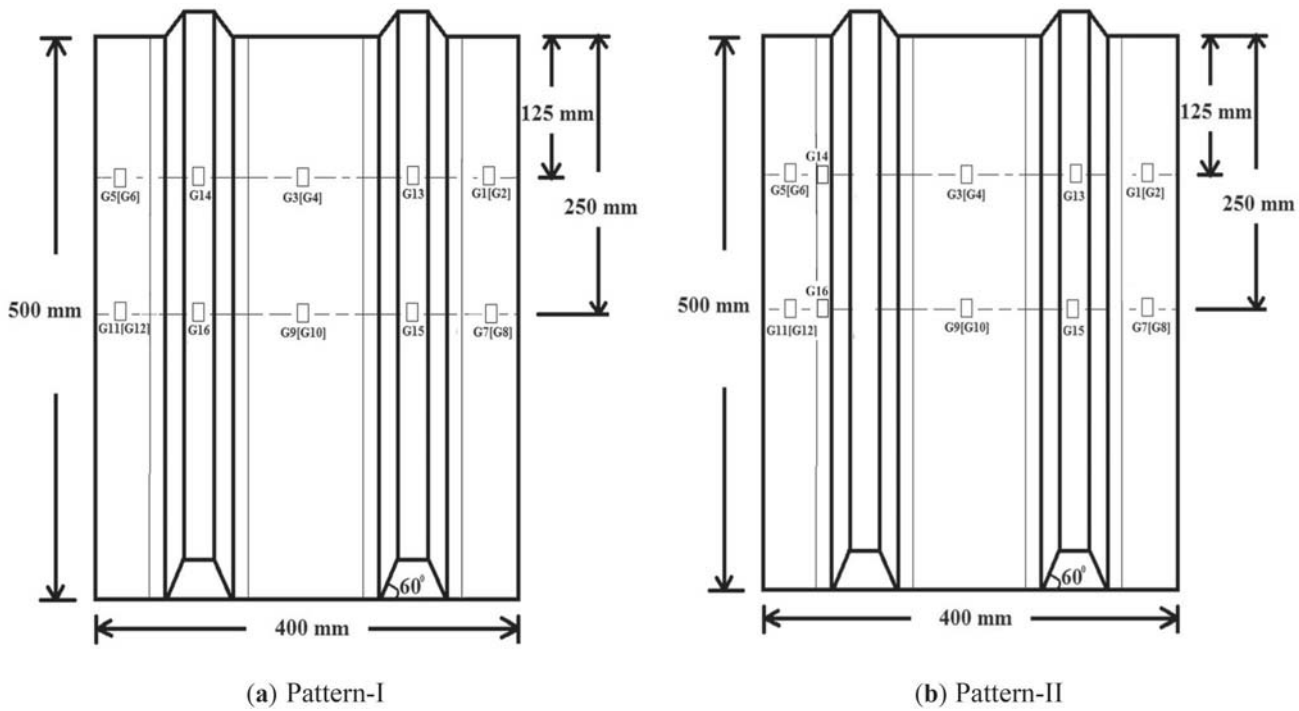

Figure 5. Locations of the strain gauges on panel.

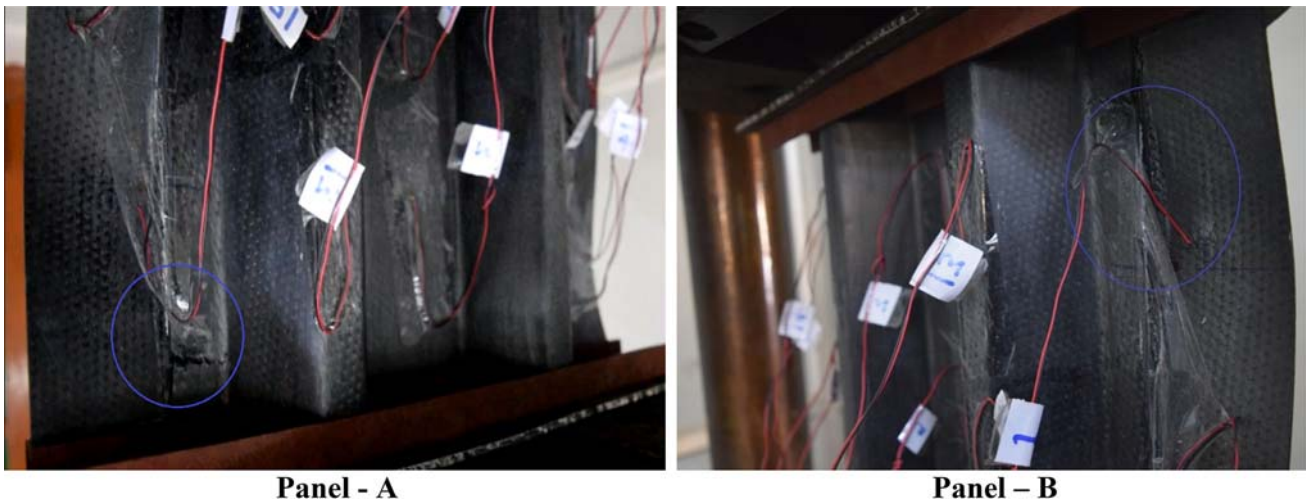

Figure 6. Failure mode of the panel.

loaded edges while the two unloaded edges of the panel were free. Before start of the experiment, the location of specimen was adjusted to confirm that the panels were uniformly loaded. The strain gauges were installed on the skin and stiffeners for monitoring the bucking status of the stiffened panel. The compressive tests were conducted with controlling the loading rate of the machine. The ideal test condition was satisfactory during the loading process; loading rate is controlled with 1 kN/s before the buckling of the hat-stiffened panel, and consequently reduced to 0.5 kN/s during the post-buckling stage. The axial displacements of the panels were noted with increasing compression load.

A FE model was developed using ABAQUS to find the first and second buckling pattern of the stiffened panel for locating the strain gauges on the hat-stiffened panel. The strain gauges were located in two patterns for the determination of behavior of skin and stiffener as shown in figure 5. Twelve strain gauges (G1–G12) were located back-to-back on both sides of the skin to determine the membrane strains and the bending strains of skin when the buckling load has been reached. Four strain gauges (G13–G16) were located on the hat-stiffener for determination of the behavior of stiffeners.

4. Experimental results

The first experiment was conducted on specimen of panel-A. The cracking sound occurred at the load of 265 kN/m, and finally, the panel collapsed at load value of 274.7 kN/m by a loud noise. A visual damage was observed near the skin-stiffener and debonding of skin-stiffener of the panel as shown in figure 6. Similar behavior was found for panel-B but failure load was obtained 304.1 kN/m which is 7.14 % more than panel-A.

Figure 7 shows the load-axial displacement curve of the compression tests on hat-stiffened panels. It is observed that the compression load increases linearly up to 196 kN/m with increasing of the axial displacement of the panel. However, at later stage, rate of load increase corresponding to the axial displacement reduces until attending the collapse load of the panels. It is evident that load carrying capacity of panel-A is lower than panel-B due to the difference of the damage locations and probably due to the manufacturing of the panel.

The strain–load curves of strain gauges (G1–G6) are presented for both stiffened panel as shown in figures 8, 9 and 10. It is observed that the strain-load curves are approximately linear but at later stage, the slope of strain-load curves converse rapidly in two opposite direction at certain load value for different back-to-back strain gauges on the panels. This certain load value can be designated as

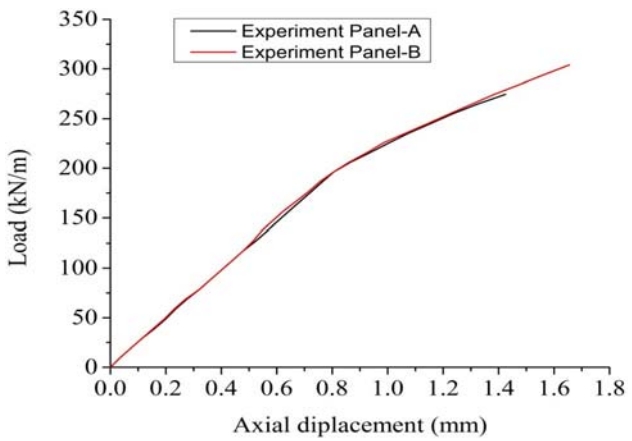

Figure 7. Load – axial displacement curves of experimental panel.

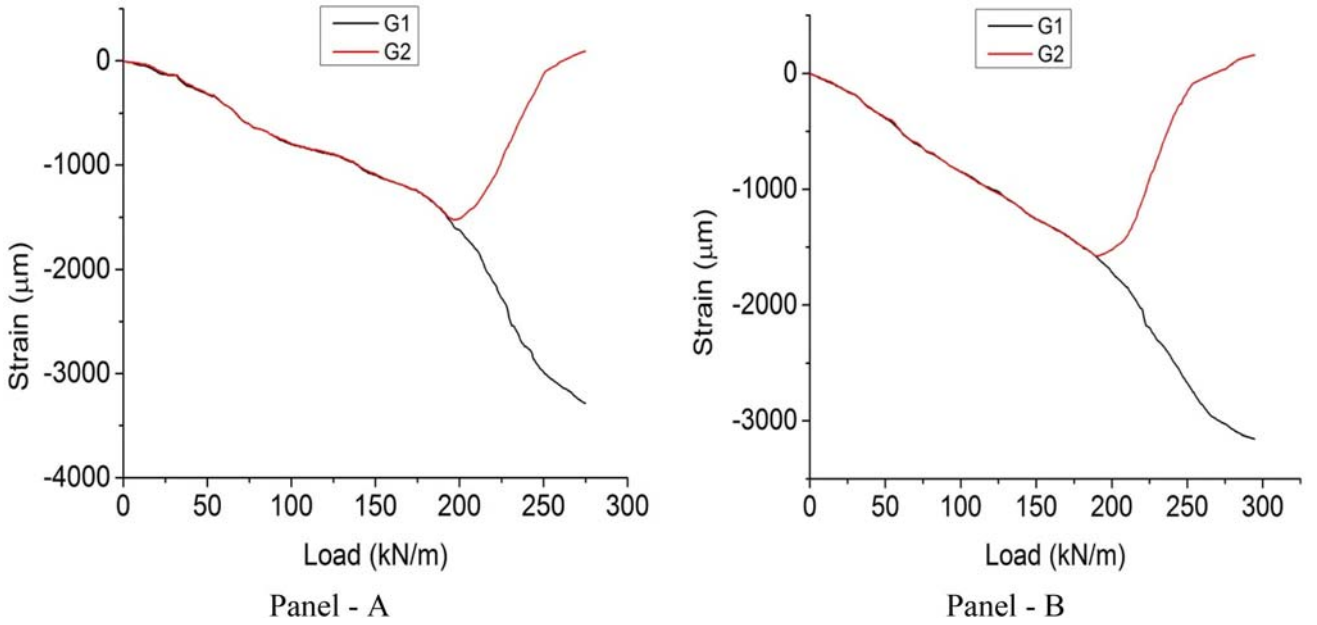

Figure 8. Strain-load curves of strain gauge G1 and G2.

the buckling load of the stiffened panel. It can be easily obtained from figures 8, 9 and 10, which value is approximately 196 kN/m in both stiffened panels. The buckling of the panel did not happen simultaneously in different position of the stiffened panel due to different damage locations, manufacturing defects of the panel and geometrical imperfections. It can be observed that the initial buckling occurred at the strain gauge located at G6 of the panel-A with a load 190.5 kN/m, and the last buckling happened at the strain gauge located on G2 of the panel-A with a compression load 196.3 kN/m. Similar buckling pattern was observed during compression test of the panel-B and it is also observed from figures 8, 9 and 10.

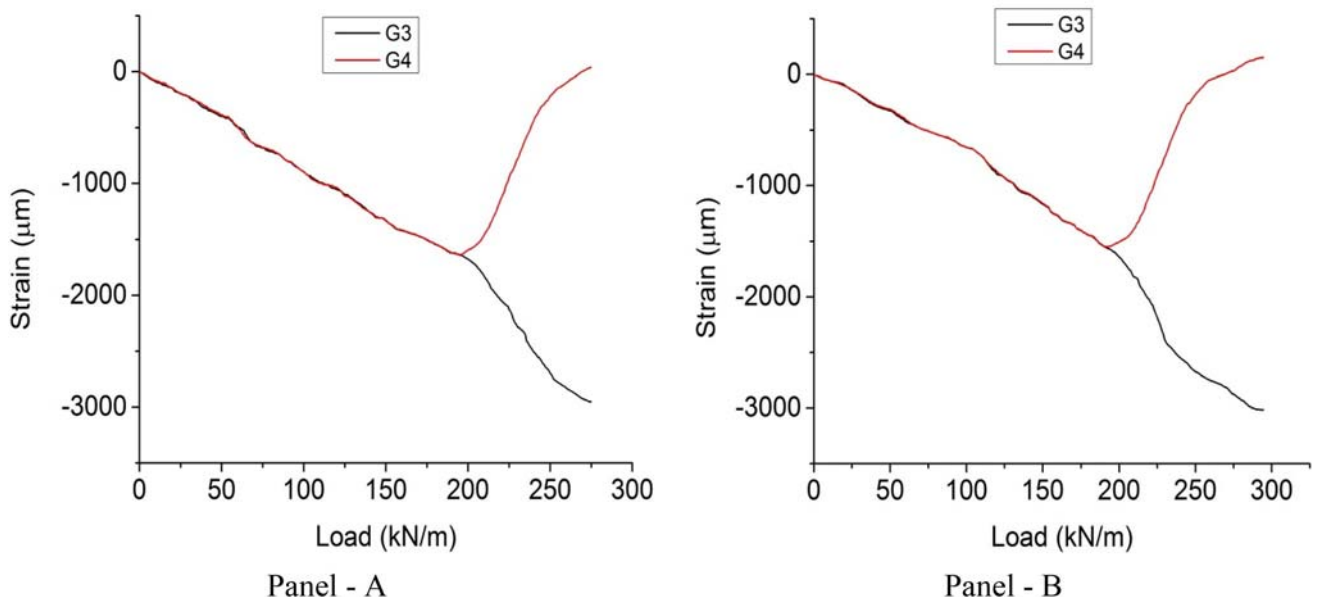

Figure 9. Strain-load curves of strain gauge G3 and G4.

Figure 11 shows the strain–load curves at different location on the panel, strain gauge G13 and G14 located at hat-stiffener upper flanges of the panel-A. However, for panel-B, G13 is located at hat-stiffener upper flanges panel-B but G14 is located at upper of skin-stiffener interface. It can be observed that the strain–load curves are slightly changed when the first buckling mode occurs. The reason behind this, the global stiffness of the laminated stiffened panel got reduced due to the local buckling of the skin. Thus, according to smeared stiffness ratio, the compression load will redistribute between plate of skin and hat-stiffeners of the panel. Hence, slopes of strain–load curves increases due to local buckling occurred near skin-stiffeners

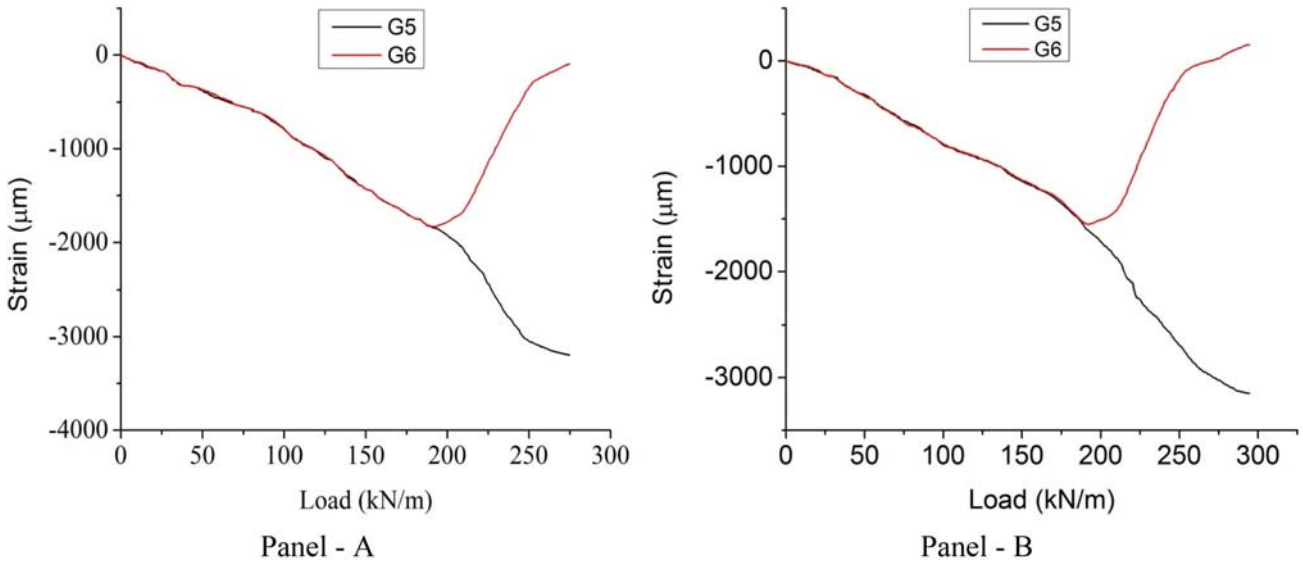

Figure 10. Strain-load curves of strain gauge G5 and G6.

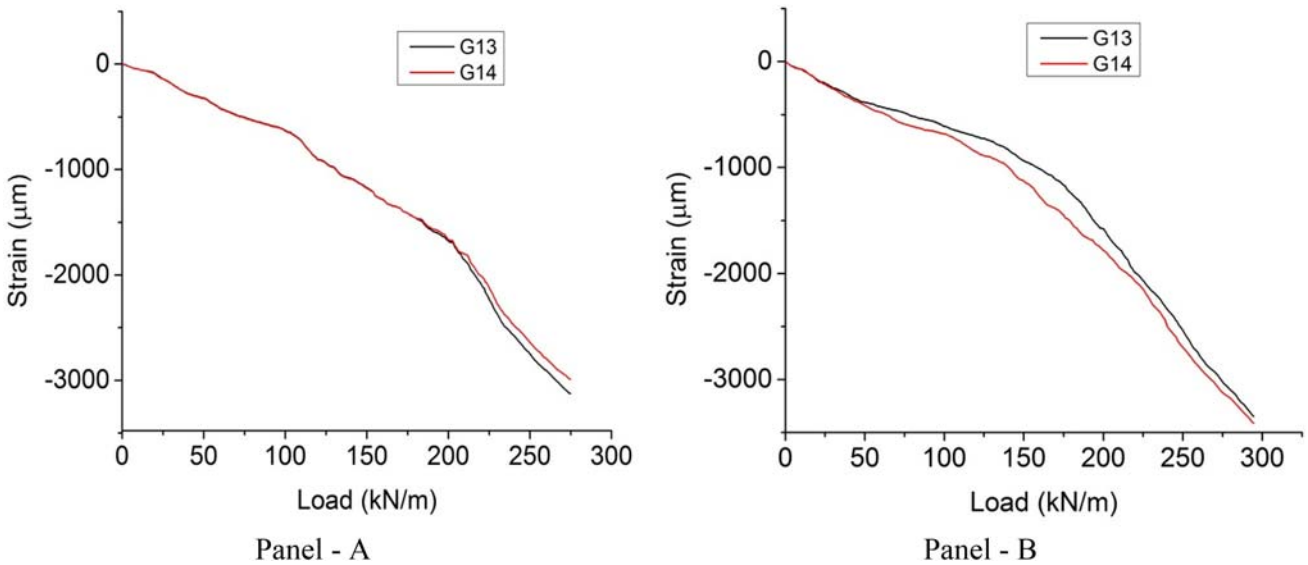

Figure 11. Strain-load curves of strain gauge G13 and G14.

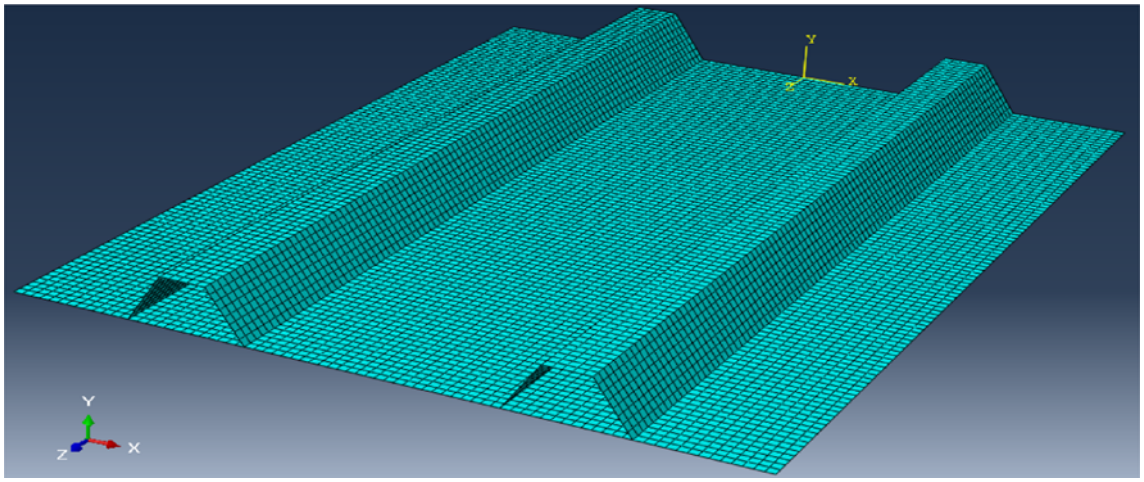

Figure 12. The panel discretized with shell element (S4R).

of the panel for strain gauges located on hat-stiffener upper flanges.

5. Non-linear FE analysis

Non-linear buckling analysis has been performed with FE model of hat-stiffened panel by using ABAQUS 6.16. Shell element S4R is considered for analysis of thin panel which has both bending and membrane capabilities. The hat-stiffened panel is discretized with small global mesh size of 5 mm and 12100 elements have bean generated for the stiffened panel as shown in figure 12. Numerical studies have been performed on laminated composite stiffened panel made with CFC of ply configuration of $[[45°/-45°/90°/0°/]_s]_s$ with 2 mm thick laminated sheet in all member of panel as shown in figure 1.

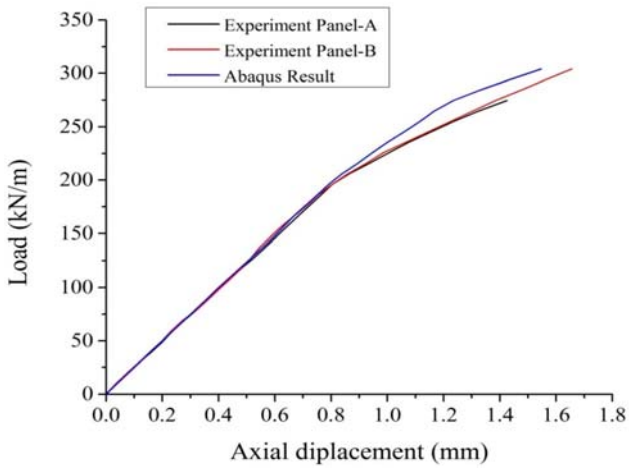

Figure 13. Load– axial displacement curves of experimental and simulated panel.

Firstly, the buckling analysis is studied using FE model to identify the buckling modes of the panel. The pre-buckling analysis is changed to perform a nonlinear FE analysis for post-buckling behavior of the panel. The post-buckling analysis has been performed with a Static Riks step in place of eigenvalue buckling step in ABAQUS. The geometric imperfections are allowed in smooth manner for the post-buckling analysis on the basis of first four Eigen value buckling modes. The panel is loaded with axial compression and clamped in loaded edges and free in unloaded edges. The model is submitted for the post-buckling analysis and monitored continuously during the progress of bucking analysis.

Hashin's failure criterion is implemented to predict the beginning of the failure in the post-buckling analysis. A stiffness reduction method [11] was applied and further increasing load initiated overall loss of stiffness, when the failure criterion is satisfied. The failure measurement is based on the fracture energy dissipated throughout damage process. The elastic properties of CFC are tabulated in table 1 for Hashin's failure criterion.

The axial displacement of the panel obtained through experiment is more than the axial displacement found from the damage model due to presence of the implanting material, such as epoxy, in the supported ends of the panel. Therefore, results are normalized using the axial displacement at the buckling load. Figure 13 shows the compression load-axial displacement curve of stiffened panel together with simulated FE model results and the experimental results. It is observed that the curve of compression load vs. axial displacement increases linearly but lateral stage it is reduced after increase of compression load. From compression load vs. axial displacement curve, the critical buckling load and critical displacement of the stiffened panel is obtained as 206 kN/m and 0.839 mm, respectively. Figure 14 shows the out of plane displacement pattern of

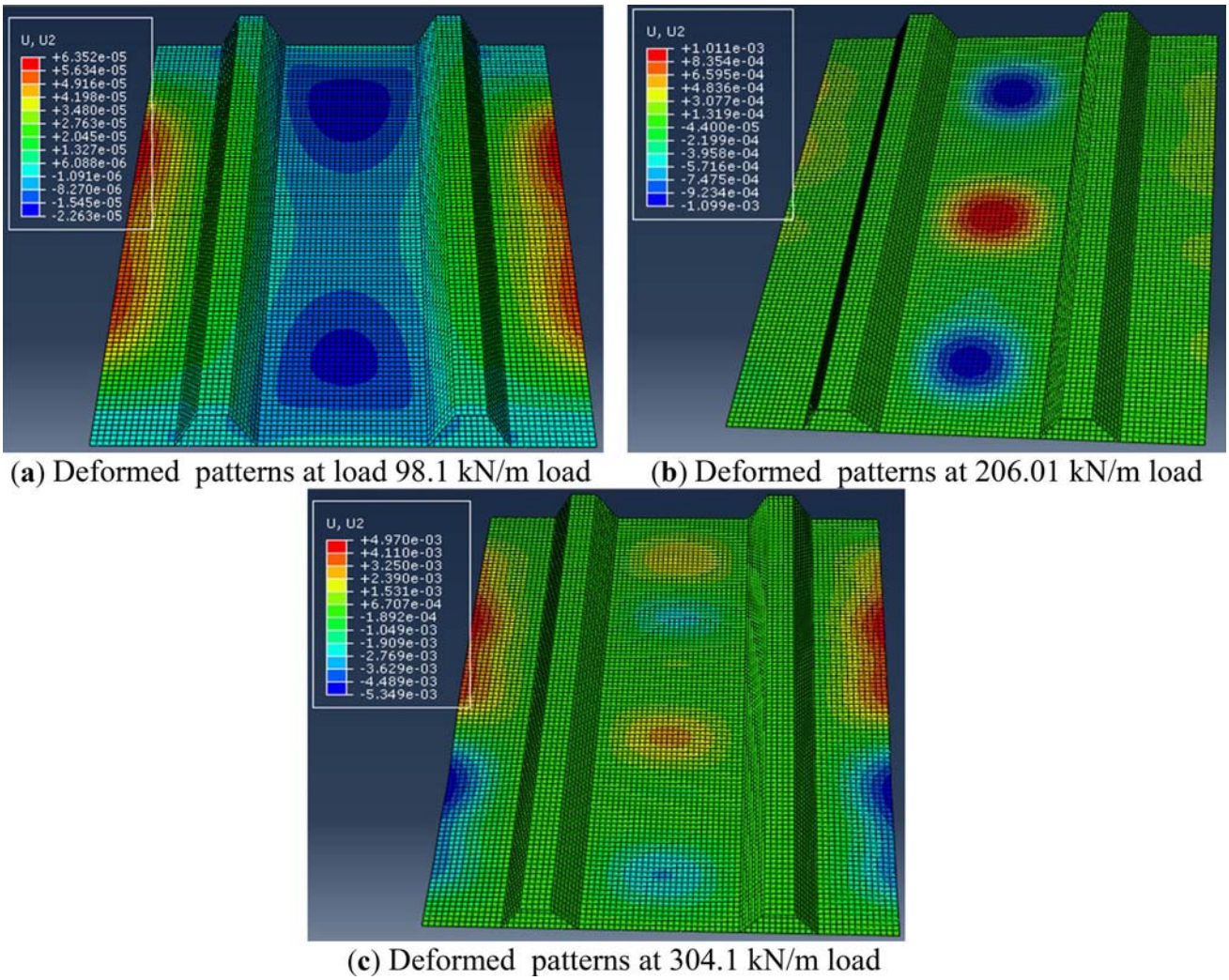

Figure 14. The out of plane displacement pattern at different load for FE analysis.

the panel at different specific loads which are taken from load-axial displacement curve as shown in figure 13. The out of plane displacement pattern shows that the compressive failure originated at edges of the panel and spreads towards skin-stiffener bonding. Finally, failure of the stiffened panel happened due to debonding between skin-stiffener.

6. Conclusions

In this work, the pre-buckling and post buckling analyses have been performed on the hat-stiffened panel under in-plane compression load by experiments and finite element simulation tool ABAQUS. The experimental results were obtained on two hat-stiffened panels with equally spaced stiffeners. The buckling behavior of the panels has been carried out with experimental study and compared with finite element model result. The following conclusions are drawn.

- The compression load-axial displacement curve of the experiments co-relates well with that of simulated FE model result for prediction of the buckling behavior of the panel up to the failure load.
- From strain analysis, the local buckling of skin has been observed before the global buckling of the panel. A damaged has been observed near the skin-stiffener and de-bonding occurred between skin-stiffener of the panel during failure of the hat-stiffened panel.
- Out of plane displacement pattern from FE analysis shows that the compressive failure originated at edges of the panel and spread towards skin-stiffener bonding, and finally failure of the panel occurs due to debonding between skin-stiffener.

References

[1] Kong C W, Lee I C, Kim C G and Hong C S 1998 Post-buckling and failure of stiffened composite panels under axial compression. *Composite Structures* 42(1): 13–21

[2] Bisagni C 2000 Numerical analysis and experimental correlation of composite shell buckling and post-buckling. *Composites Part B: Eng.* 31: 655–667

[3] Lanzi L 2004 A numerical and experimental investigation on composite stiffened panels into post-buckling. *Thin-Walled Structures* 42: 1645–1664

[4] Zhao Y and Teng J G 2004 Buckling experiments on steel silo transition junctions: II: Finite element modeling. *Journal of Constructional Steel Research* 60: 1803–1823

[5] Zhao Y 2005 Buckling behaviour of imperfect ring-stiffened cone–cylinder intersections under internal pressure. *International Journal of Pressure Vessels and Piping* 82: 553–564

[6] Bisagni C 2005 Dynamic buckling of fiber composite shells under impulsive axial compression. *Thin-Walled Structures* 43: 499–514

[7] Bisagni C and Cordisco P 2006 Post-buckling and collapse experiments of stiffened composite cylindrical shells subjected to axial loading and torque. *Composite Structures* 73(2): 138–149

[8] Gal E, Levy R, Abramovich H and Pavsner P 2006 Buckling analysis of composite panels. *Composite Structures* 73: 179–185

[9] Zimmermann R, Klein H and Kling A 2006 Buckling and post-buckling of stringer stiffened fibre composite curved panels – Tests and computations. *Composite Structures* 73(2): 150–161

[10] Pevzner P, Abramovich H and Weller T 2008 Calculation of the collapse load of an axially compressed laminated composite stringer-stiffened curved panel–An engineering approach. *Composite Structures* 83: 341–353

[11] Orifici A C, Alberdi I O D Z, Thomson R S and Bayandor J 2008 Compression and post-buckling damage growth and collapse analysis of flat composite stiffened panels. *Composites Science and Technology* 68: 3150–3160

[12] Elaldi F 2010 Structural efficiency and post-buckling strength of J- and hat-stiffened composite panels. *J. Reinf. Plast. Compos*. 29(10): 1590–1594

[13] Perret A, Mistou S, Fazzini M and Brault R 2012 Global behaviour of a composite stiffened panel in buckling. Part 2: Experimental investigation. *Composite Structures* 94: 376–385

[14] Boni L, Fanteria D and Lanciotti A 2012 Post-buckling behaviour of flat stiffened composite panels: Experiments vs. analysis. *Composite Structures* 94: 3421–3433

[15] Liu X, Hanb K, Bai R, Lei Z and Wang H 2014 Buckling measurement and numerical analysis of M-type ribs stiffened composite panel. *Thin Walled Structures* 85: 117–124

[16] Zhu S, Yan J, Chen Z, Tong M and Wang Y 2015 Effect of the stiffener stiffness on the buckling and post-buckling behaviour of stiffened composite panels – Experimental investigation. *Composite Structures* 120: 334–345

[17] SudhirSastry Y B, Budarapu P R, Madhavi N and Krishna Y 2015 Buckling analysis of thin wall stiffened composite panels. *Computational Materials Science* 96: 459–471

[18] Riccio A, Raimondo A, DiFelice G and Scaramuzzino F 2015 A robust numerical approach for the simulation of skin–stringer debonding growth in stiffened composite panels under compression. *Composites: Part B* 71: 131–142

[19] Borrelli R, Riccio A, Sellitto A, Caputo F and Ludwig T 2015 On the use of global–local kinematic coupling approaches for delamination growth simulation in stiffened composite panels. *Composites Science and Technology* 115: 43–51

[20] Wang X M, Cao W, Deng C H, Wang P Y and Yue Z F 2015 Experimental and numerical analysis for the post-buckling behaviour of stiffened composite panels with impact damage. *Composite Structures* 133: 840–846

[21] Kumar S, Kumar R, Mandal S and Rahul A K 2018 The prediction of buckling load of laminated composite hat-stiffened panels under compressive loading by using of neural networks. *The Open Civil Engineering Journal* 12: 468–480

[22] ABAQUS 2016